Journal of Biotechnology 398 (2025) 1–10

Contents lists available at ScienceDirect

Journal of Biotechnology

journal homepage: www.elsevier.com/locate/jbiotec

Assessing the role of deep eutectic solvents in *Yarrowia lipolytica* inhibition

Filipe S. Buarque [a,b,*], Bernardo D. Ribeiro [a], Mara G. Freire [b], Maria A.Z. Coelho [a], Matheus M. Pereira [c,**]

[a] *Biochemical Engineering Department, School of Chemistry, Federal University of Rio de Janeiro, Brazil*
[b] *CICECO-Aveiro Institute of Materials, Department of Chemistry, University of Aveiro, Portugal*
[c] *University of Coimbra, CERES, Department of Chemical Engineering, Rua Sílvio Lima, Pólo II – Pinhal de Marrocos, Coimbra 3030-790, Portugal*

A R T I C L E I N F O

Keywords:
Microorganism inhibition
Hexokinase
Alternative solvents
Enzymatic tunnels
Molecular docking

A B S T R A C T

Yarrowia lipolytica has gained recognition as a microorganism with biological relevance and extensive biotechnological applications. Some of its features include a high enzyme secretion capacity and a high cell-density fermentation mode. Hexokinase (YlHxk) is a vital enzyme in *Y. lipolytica* growth since it catalyzes glucose metabolism through phosphorylation in the glycolytic pathway. Given the potential application of deep eutectic solvents (DES) as novel solvents in biotechnological processes, this study evaluated the influence of eighteen DES on the growth of *Y. lipolytica*. Furthermore, this work examined the effects of individual ions on the YlHxk enzyme by analyzing its enzymatic tunnel structure, molecule transport, and molecular docking. The results revealed a significant reduction in yeast growth in the presence of most DES compared to the control (medium without DES), with the exception of the $[N_{8881}]$Cl: hexanoic acid (1:1) DES. The growth varied between 11.95 ± 0.60 and 0.68 ± 0.17 g dry cell weight L^{-1}. According to the enzymatic tunnel analysis, DES components associated with the lowest microbial growth values were transported through tunnel 1. On the other hand, DES components had their pathway facilitated through tunnel 2 ($[N_{8881}]^+$ and hexanoic acid) and showed growth values close to the control. Molecular docking analysis identified a similarity between all the ligands in this tunnel (including substrate and product), presenting binding interactions with the ASN273 amino acid of the YlHxk active site. Combining experimental results with computational tools provided promising insights at the molecular level, while also potentially reducing analysis costs and time, paving the way for similar approaches in broad biocatalytic reactions.

1. Introduction

Yarrowia lipolytica is classified as an unconventional yeast, being regarded by the FDA (Food and Drug Administration) as GRAS (Generally Regarded as Safe), which has been widely studied due to its high capacity to produce different biocatalysts of industrial interest, such as lipases, proteases, esterases, among others (Barth and Gaillardin, 1997; Nicaud, 2012; Buarque et al., 2023a). This yeast can degrade several hexoses, such as glucose, fructose, and mannose. These hexoses are transported inside the cell via hexose transporters and incorporated into the central carbon metabolism after their phosphorylation by hexose kinases (Hapeta et al., 2021a, 2021b). Hexokinase (YlHxk) is the first glycolytic pathway enzyme responsible for catalyzing the transfer of a phosphoryl group from ATP to glucose to form glucose 6-phosphate and ADP (Kuser et al., 2000).

Biotechnological processes can be performed by both whole cells and isolated enzymes. The use of whole-cell catalysts has some advantages, such as allowing cofactor regeneration, providing a natural environment and avoiding enzyme denaturation and inactivation that can occur under adverse conditions, including unconventional (*i.e.*, nonaqueous) conditions. The combination of whole-cell catalysts and unconventional reaction media containing organic solvents is highly attractive, especially for hydrophobic substrates (Yang et al., 2017; Maugeri and Domínguez De María, 2014; Panić et al., 2021; Pätzold et al., 2019). Within this context, a potentially greener alternative to conventional organic solvents are deep eutectic solvents (DESs), which have received special attention due to their promising physicochemical properties if properly designed, such as low volatility, low vapor pressure, high thermal stability, biocompatibility, biodegradability, and nonflammability (Yang et al., 2017; Pätzold et al., 2019).

* Corresponding author at: Biochemical Engineering Department, School of Chemistry, Federal University of Rio de Janeiro, Brazil.
** Corresponding author.
E-mail addresses: filipesmith@eq.ufrj.br (F.S. Buarque), matheus@eq.uc.pt (M.M. Pereira).

https://doi.org/10.1016/j.jbiotec.2024.11.016
Received 26 July 2024; Received in revised form 14 November 2024; Accepted 25 November 2024
Available online 28 November 2024
0168-1656/

DES can be defined as the association of two or more compounds by strong hydrogen-bonding, involving at least one hydrogen bond acceptor (HBA) and one hydrogen bond donor (HBD). The term designer solvents has been used to describe one of the DES's main advantages: their physicochemical properties can be tailored by selecting different chemical structures of the DES components at different proportions. This tuning could be applied to biocatalysis to modulate/design specific solvents to direct the route of a reaction to obtain a target product, increase enzyme activity or stability, and/or increase reaction yield (Panić et al., 2021; Buarque et al., 2023b).

An important requirement for successfully applying DES in a whole-cell process is low toxicity towards the microorganism. The biological effects exerted by these green solvents on microbial cells will typically depend on the organism's nature, synergistic interactions in the chemical structure, hydrophobicity, polarity, viscosity, and hydrogen bond basicity/acidity, molar ratio, among other properties (Gao et al., 2015; Zhao, 2016; Toledo et al., 2019; Santos et al., 2014). For example, Yang et al (Yang et al., 2017). reported the impact of 45 DES based on choline chloride (ChCl) and organic acids, alcohols or sugars on the bioconversion of isoeugenol to vanillin catalyzed by *Lysinibacillus fusiformis* CGMCC1347 cells. It was demonstrated that aqueous media containing DES improved conversion yields up to 142 % when compared to those obtained in DES-free aqueous systems. Qian et al (Qian et al., 2023). described a 63 % increase in the yield of chiral aryl alcohol biosynthesis by enhancing cell permeability, overcoming mass transfer limitations during the reduction of prochiral ketones. This was achieved using whole cells of *Geotrichum candidum* ZJPH1907 and a medium containing DES composed of ChCl and amino acids. Chlipała et al (Chlipała et al., 2024). applied *Y. lipolytica* KCh 71 yeast as a biocatalyst in an aqueous DES solution (ChCl combined with a sugar or polyol) for the bioreduction of 4′-hydroxychalcone (trans-1). It was achieved a bioconversion rate of 70 % after 24 h, representing a five-fold increase compared to the results obtained in the media without DES. However, to our knowledge, the impact of DES-based solvents on microbial growth has not been investigated. Furthermore, the many possible combinations of DES-forming components and interactions with the enzyme sites make the molecular-level understanding challenging to address experimentally.

In silico approaches can provide relevant data for understanding the pathways and possible interactions of inhibitors and/or activators with the amino acids in enzyme tunnels. The ability to predict molecular interactions and the routes for substrates and/or specific molecules into these tunnels toward the active site could promisingly facilitate experimental methodologies, optimizing time and costs (Barbosa et al., 2019a; Bisht et al., 2017). The online server CaverWeb 1.0 is a virtual screening tool widely used to identify and analyze transport tunnels in macromolecular structures (Kim et al., 2024). Furthermore, this computational method provides users with intuitive, simple, and fast tunnel analysis (Filipovic et al., 2020). Tunnels control the passage of ligands, such as substrates, products, water molecules, and solvents towards the enzyme's active sites (Chong et al., 2023). Although tunnels have varied structures and functions, the knowledge of their properties is crucial to understanding better the transport specificity of substrates and ligands (Kaushik et al., 2018; Azevedo et al., 2022). Stourac et al (Stourac et al., 2019). demonstrated that tunnels and their properties can define many important protein characteristics, like substrate specificity, enantioselectivity, stability, and enzyme activity.

Another computational method is molecular docking, a tool used to predict the binding affinity of the receptor-ligand complex due to its ability to accurately predict the ligand conformation with amino acids from the active sites of protein structures. The main goal of molecular docking is to computationally simulate the receptor-ligand complex and accomplish an optimized conformation so that the free energy of the overall system is minimized (Rodrigues et al., 2021, 2024; Ferreira et al., 2015). Toledo et al (Toledo et al., 2019)., through molecular docking, evaluated the influence of HBAs (choline chloride, choline dihydrogen phosphate, choline dihydrogen citrate, and betaine) and HBDs (ethylene glycol, glycerol, erythritol, and xylitol) combined in DES on reactions catalyzed by isolated laccase. The study demonstrated that most DES constituents form hydrogen bonds between receptors and amino acids. However, ligands with higher affinity energy values lead to improved laccase activity.

In this study, we evaluated the DES effect on *Yarrowia lipolytica* growth. To this purpose, a series of DES formed by combining six hydrogen bond acceptors (HBA) and three hydrogen bond donors (HBD) was evaluated. The HBAs selected include: tetraoctylammonium chloride - $[N_{8888}]Cl$, methyltrioctylammonium chloride - $[N_{8881}]Cl$, methyltrioctylammonium bromide - $[N_{8881}]Br$, tetrabutylammonium chloride - $[N_{4444}]Cl$, tetrabutylammonium bromide - $[N_{4444}]Br$, and choline chloride - ChCl. HBDs used were: hexanoic, octanoic, and decanoic acids. Understanding the molecular-level mechanisms of these alternative solvents' impact on cell growth or inhibition is essential in biocatalysis. Thus, computational tools to analyze the interactions between DES components and the yeast enzyme hexokinase (YlHxk) were additionally applied.

2. Materials and methods

2.1. Materials

The DES constituents, viz. $[N_{8888}]Br$, $[N_{8881}]Cl$, $[N_{8881}]Br$, $[N_{4444}]Cl$, $[N_{4444}]Br$ and ChCl, as well as the hexanoic, octanoic and decanoic acids, were supplied by Sigma-Aldrich with a purity >98 wt%. The culture medium components used were bacterial peptone, purchased from Oxoid; yeast extract, purchased from Sigma-Aldrich; and glucose (purity >98 %), supplied by Vetec. The chemical structures of the investigated DES are given in Fig. 1.

2.2. Preparation of DES

The eighteen DES investigated in this work were prepared by the heating method by mixing the respective HBA ($[N_{8888}]Br$, $[N_{8881}]Cl$, $[N_{8881}]Br$, $[N_{4444}]Cl$, $[N_{4444}]Br$, ChCl) and HBD (hexanoic acid, octanoic acid, and decanoic acid) in sealed glass vials at 1:1 molar ratio. The mixtures were placed under constant heating (80 °C) and stirred for 1 h (Buarque et al., 2023b; Shishov et al., 2022). Aqueous solutions at 20 wt % were then prepared for each DES.

2.3. Yarrowia lipolytica growth on the DES presence

A wild strain of *Y. lipolytica* (IMUFRJ 50682), isolated from an estuary of Guanabara Bay in Rio de Janeiro and stocked at 4 °C in YPD-agar medium (1 % yeast extract, 2 % peptone, 2 % glucose, and 3 % agar) (Hagler and Mendonqa-Hagler, 1981), was used in this work.

To obtain an inoculum, yeast cells were grown in Erlenmeyer flasks (0.5 L) containing YPD (1 % yeast extract, 2 % peptone, 2 % glucose) medium (0.2 L) at 28°C on a rotary shaker (160 rpm) for about 72 h. Then, cell concentration in g dry cell weight L^{-1} was determined at 570 nm (Santos et al., 2022). 1 g p.s. L^{-1} of yeast was resuspended and inoculated into a new YPD culture medium (0.02 L) containing 20 wt% of DES in Erlenmeyer flasks (0.05 L) for cell growth at 28 °C, 250 rpm, and for 48 h. All materials needed for the experiments were autoclaved at 1 atm for 25 min. It is important to mention that the addition of DES to microbial growth did not increase the culture's turbidity or decrease the medium's pH.

2.4. Computational analysis

2.4.1. Structural analysis of Hexokinase from Yarrowia lipolytica (YlHxk)

To precisely identify the active site of *Yarrowia lipolytica* hexokinase (YlHxk), we based ourselves on the study by Zeng et al (Zeng and Fromm, 1995). that provides a detailed analysis of the amino acids

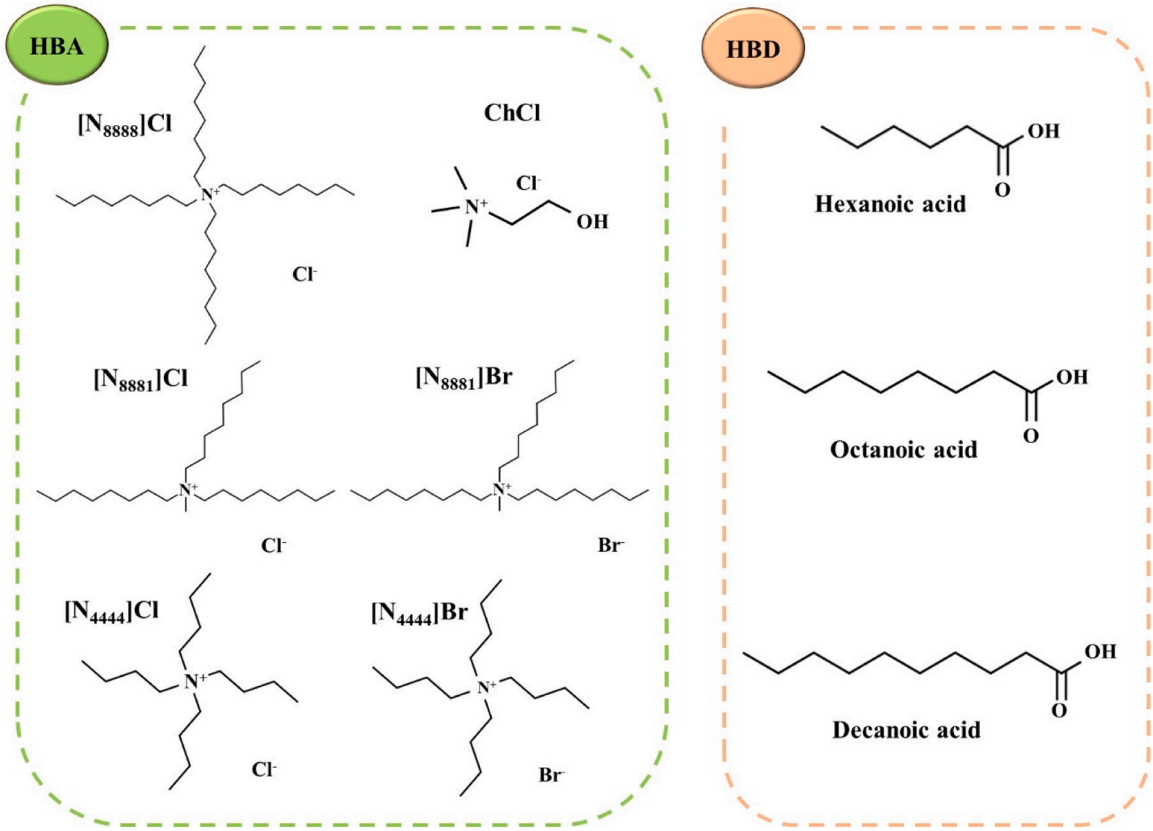

Fig. 1. : Chemical structures of the DES-forming hydrogen bond acceptors (HBAs) and donors (HBDs).

constituting the catalytic site of human hexokinase. Human and *Y. lipolytica* hexokinase share high structural and functional homology, allowing the conclusions learned from the human structure to be applied to our study. Using the amino acid sequence and three-dimensional structure of human hexokinase as a reference, a homology comparison with the structure of YlHxk was carried out, revealing that residues Asn246, Asp247, Thr270, Asn273, Thr298, and Glu338 are the amino acids involved in the yeast catalytic site.

The allosteric sites were identified using the PASSer model, which performs a detailed analysis of the dynamic and structural characteristics of the enzyme to identify potential allosteric sites. PASSer offers three models based on machine learning: an ensemble model consisting of extreme gradient boosting (XGBoost) and a graph convolutional neural network (GCNN), an automated machine learning model powered by AutoGluon from Amazon Web Services (AWS), and a learning model for classification (LTR). The LTR algorithm, predetermined with LightGBM, is able to classify the pockets in order of their probability of becoming the main allosteric sites (Huang et al., 2011; Xiao et al., 2023; Lu et al., 2019a).

2.4.2. Tunnels calculation

The computational analysis was performed using the online server CaverWeb V1.0 (https://loschmidt.chemi.muni.cz/caverweb). The YlHxk tunnels were identified using the default configuration, and then filtered based on their bottleneck radius (Å) and length (Å). Then, the binding energies: bound state (E_{bound}), maximum energy barrier (E_{max}), unbound state ($E_{surface}$), binding energy barrier (E_a) and difference in energy of the bound and unbound states (ΔE_{BS}) were calculated for each ligand (substrate, product and solvents). The results obtained were visualized and analyzed using Discovery Studio v21 (Accelrys, San Diego, CA, USA) (Vavra et al., 2019; Buarque et al., 2023c).

2.4.3. Molecular docking

The interactions of Hexokinase from *Yarrowia lipolytica* (YlHxk) with all HBAs and HBDs were calculated using the AutoDock Vina 1.1.2 program (Trott and Olson, 2010). The molecular docking analysis used the crystal structure of YlHxk (UniProt: F2Z672) as a receptor. Auto DockTools (ADT) was used to prepare the enzyme input file. Ligands 3D structures (HBA, HBD, substrate and product) were created using Discovery Studio v21 (Accelrys, San Diego, CA, USA) and applied to the Chem3D-MM2 protocol for energy minimization to create the ligand files (Buarque et al., 2023c). Then, AutoDockTools (ADT) (Morris et al., 2009) was used to convert all ligand into input files (pdbqt), setting all possible rotatable bonds defined as active by torsions, and convert the YlHxk PDB file into.pdbqt input files. The coordinates at the center of the grid box (x-, y-, and z-axes) were $1.484 \times 0.507 \times 1.649$. The grid dimension was 80 Å × 80 Å × 90 Å to cover the whole YlHxk structure. The model with the lowest docking score was obtained using the following configuration: *exhaustiveness* = 100, *num_modes* = 10 and *seed* = 100.

2.5. Statistical analysis

All experiments were carried out in triplicate, and results were presented as the mean ± standard deviation. The experimental data were analysed using the Statistica 8.0 software. A Tukey's honestly significant difference (HSD) test compared treatment means, and ANOVA established their significance. Differences of $P \geq 0.05$ were considered statistically significant.

3. Results and discussion

3.1. Cell growth in DES-containing media

In the literature (Santos et al., 2014; Mohedano et al., 2022; Pernak et al., 2003), it has been shown that microorganisms can tolerate specific amounts of solvents in their culture media. Nevertheless, to our knowledge, DES behavior in the *Yarrowia lipolytica* yeast growth has not yet been explored. Fig. 2 shows the microbial growth kinetics in the DES presence at a 20 wt% concentration and the control, formed by YPD medium only (yeast extract, peptone, and dextrose). For a better overview and understanding analysis, the DES were divided into two sets based on the type of halide ion in the HBA: chloride-based (Fig. 2a) and bromide-based (Fig. 2b). Table S1 in Supporting Information offers a detailed breakdown of the cell growth values for each DES components alongside their corresponding pH levels. In general, there was a significant reduction in yeast growth in the DES-based solvents' presence compared to the control (medium without DES), with the exception of DES consisting of $[N_{8881}]Cl$ + hexanoic acid.

The kinetic growth profile showed similar behaviour, and the exponential phase lasted until 20 h, followed by a deceleration phase until 24 h. Subsequently, another phase of accentuated growth was observed, reaching the peak of microbial growth at 32 h, and finally a phase of decay in growth rates was observed. The growth rates for the medium containing DES-$[N_{8881}]Cl$ + hexanoic acid ranged from 0.37 ± 0.11–11.95 ± 0.96 g dry weight of cells L^{-1}, while the control varied from 0.37 ± 0.11–13.12 ± 1.09 g dry weight of cells L^{-1}. This indicates a broad range of inhibitory effects depending on the specific DES combination. The inhibitory effect on cell growth varied according to the type of HBA used in the DES. The order of decreasing cell growth was observed as follows: $[N_{8881}]Cl$ > $[N_{4444}]Cl$ > ChCl > $[N_{8888}]Br$ > $[N_{8881}]Br$ > $[N_{4444}]Br$. This sequence shows that chloride-based HBAs ($[N_{8881}]Cl$, $[N_{4444}]Cl$, and ChCl) were less inhibitory compared to bromide-based ones. Among the bromide-based HBAs, an interesting observation was noted with the DES composed of $[N_{8881}]Br$ + hexanoic acid. This specific combination resulted in intermediate cell growth values due to the influence less detrimental of the cation.

Regarding the HBD component, cell growth decreased as the length of the fatty acid alkyl chain increased: hexanoic > octanoic > decanoic acids. This trend suggests that shorter-chain fatty acids like hexanoic acid are less inhibitory to *Y. lipolytica* growth compared to longer-chain fatty acids. The results emphasize that bromide-based DESs generally exert a stronger inhibitory effect on cell growth compared to chloride-based DESs. This is likely due to the lower hydrogen bond basicity (β) of bromide ions in comparison to chloride ions. The hydrogen bond basicity of anions influences how they interact with cellular components. Some authors (Li and Sen, 1998; Van Lam Van et al., 2021; Matoba et al., 2021) have shown that increasing the basicity of culture medium components can enhance catalytic activity within cells. High basicity molecules tend to diffuse into the enzyme core, potentially

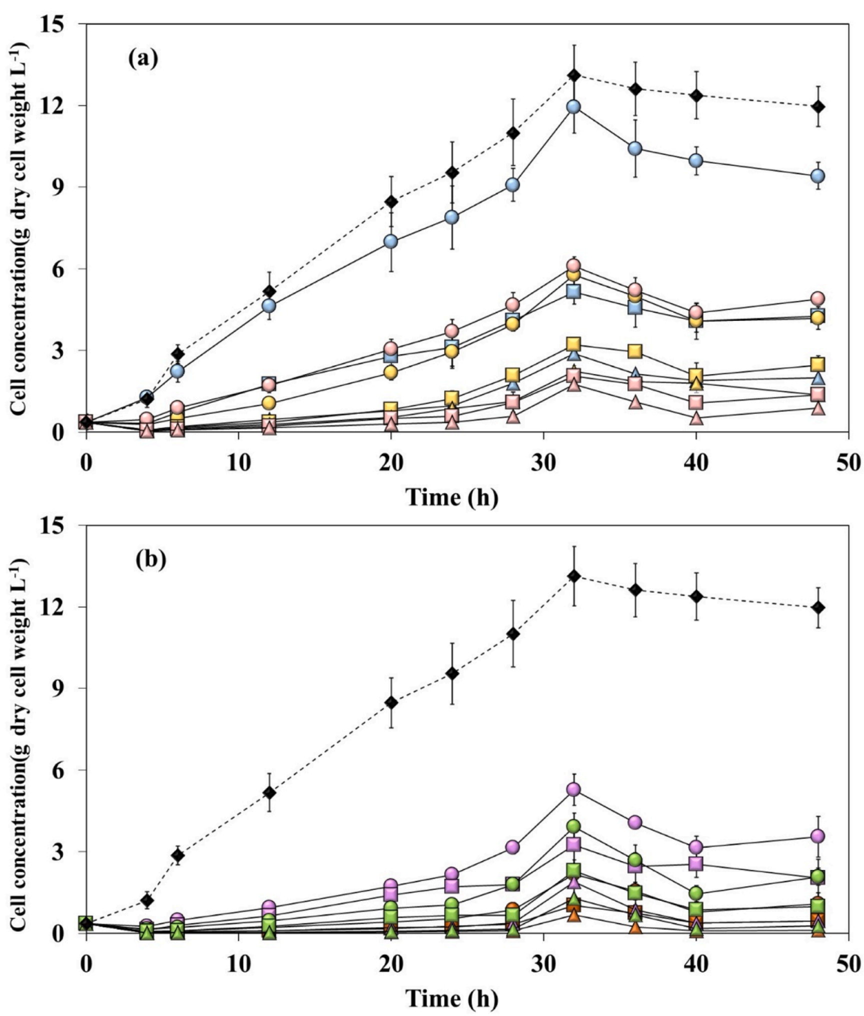

Fig. 2. : *Yarrowia lipolytica* kinetic growth profile in the presence of deep eutectic solvents (DES) formed by ammonium salts (colors) + fatty acids (hexanoic acid – C_6 (●), octanoic acid – C_8 (■), and decanoic acid – C_{10} (▲)) at 20 wt%: (a) $[N_{8881}]Cl$ - light blue, $[N_{4444}]Cl$ - yellow, and ChCl - light pink; (b) $[N_{8881}]Br$ - purple, $[N_{4444}]Br$ - light green, and $[N_{8888}]Br$ - orange. Control - black, dotted lines.

disrupting intramolecular hydrogen bonds, leading to enzyme denaturation and reduced cell viability. This phenomenon corroborates the results found for DES comprising bromide ions, having lower β values, and thus a more profound negative impact on cell growth compared to their chloride DES counterparts.

Santos et al (Santos et al., 2014). evaluated choline-based ionic liquids (ILs) toxicity on *Saccharomyces cerevisiae*, *Yarrowia lipolytica*, and *Kluyveromyces marxianus* yeast. According to the results, choline acetate and chloride choline showed inhibitions at concentrations of 3.2 and 6.25 %, respectively, compared to the YPD control medium. These findings support the complex interplay between DES components and microbial cell growth, emphasizing the need for careful selection of DES components in biotechnological applications to avoid inhibitory effects on microbial processes.

To obtain insights into the molecular behavior of these solvents and their interactions, a detailed molecular dynamics (MD) analysis was conducted. This analysis focused on identifying enzymatic tunnels and elucidating the chemical interactions between the DES and hexokinase, a critical enzyme in yeast metabolism.

3.2. Computational analysis

3.2.1. YlHxk structure

YlHxk is a globular enzyme of around 50 kDa, composed of 534 amino acids. It is codified by the YlHXK1 gene (YALI0B22308g), which has 2041 base pairs and a K_m of 0.38 mM with glucose. The YlHxk structure reveals a central catalytic site, formed by six amino acids: Asn246, Asp247, Thr270, Asn273, Thr298, and Glu338, as shown in Fig. 3.

In addition to the catalytic site, YlHxk has three allosteric sites (Fig. 3), as predicted by the PASSer server (Protein Allosteric Sites Server, https://passer.smu.edu) (Xiao et al., 2022; Tian et al., 2023). PASSer is a robust web tool designed to predict allosteric sites on proteins, ranking them based on the probability of being functional allosteric sites. The probabilities of sites 1, 2, and 3 being the main site are 45.19 %, 40.57 %, and 31.88 %, respectively. Allosteric site 1 (blue, Fig. 3) includes the amino acids: SER79, Gly80, Asp100, Arg157, Pro169, Arg165, Thr98, Ser168, Gln161, Ala160, Lys167, Thr164, Pro170, Asp166, Phe163, Leu99, and Asp156. The amino acids in allosteric site 2 (green, Fig. 3) are: Tyr195, Asp460, Asp247, Lys212, Arg209, Gln208, Thr270, Glu338, Ile267, Asp62, Glu305, Gly213, Arg331, Val272, Asn273, Asn246, and Tyr345. While the amino acids that constitute allosteric site 3 (orange, Fig. 3) are: His172, Asp154, Arg157, Ile184, Pro171, His185, Asn173, Pro170, Gln174, Ile176, Lys519, and Asp156.

3.2.2. Dynamics of ligand transport through YlHxk tunnels

Understanding the behavior of ligands within the enzymatic tunnel's structures through the in-silico analysis is crucial for advancing biocatalysis. Enzymatic tunnels are pathways within the enzyme structure that guide substrates to the active site and products away from it (Azevedo et al., 2022; Stourac et al., 2019; Planas-Iglesias et al., 2021) Through molecular dynamics simulations, eight potential tunnels within the hexokinase enzyme structure were identified, as shown in Fig. 4. However, four tunnels presented unfavorable substrate, product, and ligand transportation characteristics. This is due to the dimensions of the enzymatic channel not being suitable or for some other not known reasons. These tunnels have been classified by CaverWeb 1.0 as having low throughput, meaning they are less important than others for transport. Therefore, it is unlikely to be functionally relevant for transporting the respective ligands (Stourac et al., 2019; Pravda et al., 2014).

According to Fig. 4, the lengths of the tunnels ranged between 4.8 and 15.2 Å, and throughput values varied from 0.81 to 0.91. Moreover, tunnels 1 and 2 have also been demonstrated to have a larger bottleneck radius (tunnel 1: 2.7 Å, tunnel 2: 2.6 Å, tunnel 3: 1.8 Å, and tunnel 4: 1.8 Å). Given the above, it is suggested that tunnels 1 and 2 allow for a lower energy barrier and facilitate the transport of substrate and product to the hexokinase active site. Throughputs near 1.0 indicate a higher likelihood that the tunnel is effectively used as a route for the transport of substances, which is a crucial factor for efficient enzymatic reactions (Kaushik et al., 2018). The larger bottleneck radius and shorter length of tunnels 1 and 2 suggest that these tunnels may offer a lower energy barrier for the transport of substrates and products of the hexokinase active site. This is supported by findings from Chovancova et al (Chovancova et al., 2012). and Marques et al (Marques et al., 2017)., who demonstrated that channels with larger neck radii and shorter lengths facilitate better ligand transport and enhance biocatalytic efficiency. This is because these structural features promote faster ingress and egress of molecules, thereby improving the enzyme's overall catalytic throughput. Lu et al (Lu et al., 2019b). observed that shorter tunnels in S7-xyl xylanase (PDB: 2UWF) led to better product release and enhanced relative activity of the enzyme. This aligns with our findings, where the shorter and wider tunnels (tunnels 1 and 2) in hexokinase are likely contributing to more efficient catalytic processes.

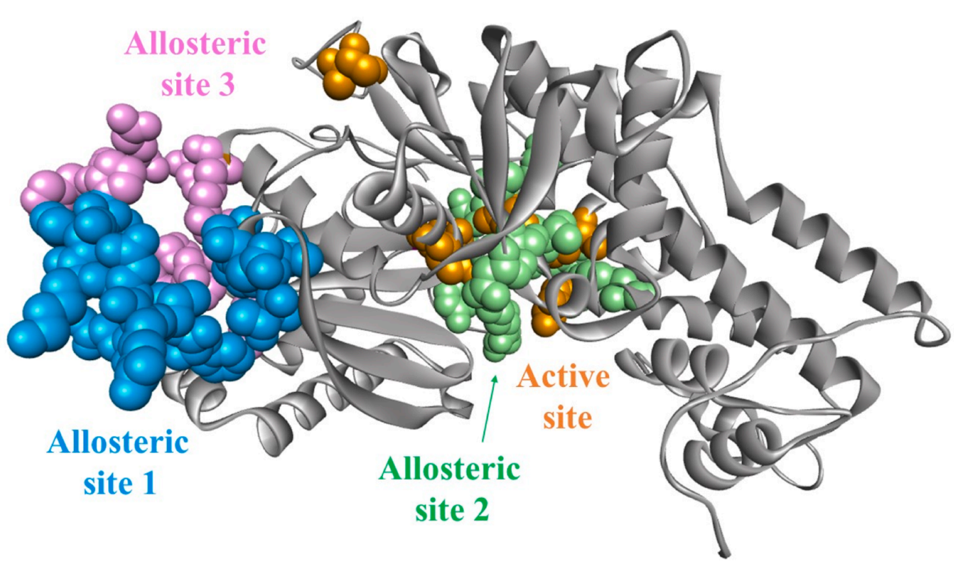

Fig. 3. **:** Three-dimensional structure of *Yarrowia lipolytica* hexokinase (YlHxk) (UniProt: F2Z672) with catalytic and allosteric sites identified: catalytic site (orange), allosteric site 1 (blue), allosteric site 2 (green) and allosteric site 3 (pink).

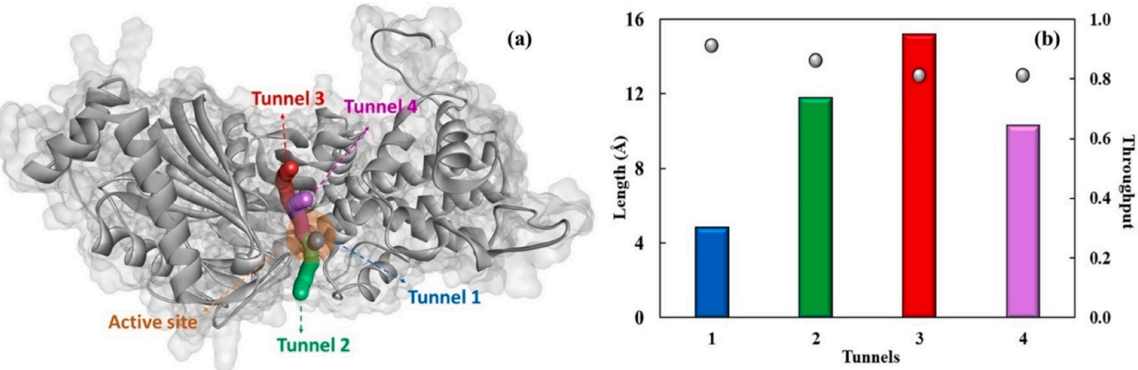

Fig. 4. **:** Hexokinase from *Yarrowia lipolytica* (YlHxk) (UniProt: F2Z672): (a) YlHxk structure and tunnels enzymatic identify: tunnel 1 (blue), tunnel 2 (green), tunnel 3 (red), and tunnel 4 (purple); (b) comparative analysis of length and throughput along tunnels with the highest transport probability.

The energy values (E_{bound}, E_{max}, $E_{surface}$, E_a, and ΔEBS, in kcal·mol^{-1}) through tunnels 1–4 at the input and output were calculated (Table S2 and S3 in Supporting Information) aiming to analyze in which channel these substances are most likely to pass through to better understand the DES impact on the inhibition of the enzyme responsible for microbial growth. In summary, E_{bound} is the minimum energy associated with the binding of the ligand to the active site. E_{max} is the maximum binding energy of the ligand within the tunnel. $E_{surface}$ is the minimum energy of the ligand bound at the enzymatic surface, whereas E_a is the minimum energy for converting substrate into product. ΔEB, given by the difference between $E_{surface}$ and E_{bound}, corresponds to the energy difference between the ligand bound at the surface and active sites (Vavra et al., 2019; Prokop et al., 2012; Chaudhary and Mishra, 2016). The ligand transport potential in tunnels can be analyzed using E_{max} and E_a. The lowest E_a values (close to 0) associated with negative E_{max} values indicate a higher probability of the ligand passing through the tunnel to the active site (Singh et al., 2021; Pinto et al., 2021).

The results indicate that most of the HBA-forming cations, i.e. $[N_{8888}]^+$, $[N_{4444}]^+$, and $[Ch]^+$, with some HBDs (octanoic acid and decanoic acid) are more likely to be transported (input and output) to tunnel 1, as seen in Figure S1, and Table S2 and S3 (in Supporting Information). These constituents exhibited the highest inhibitory effects on YlHxk. The exception was $[N_{8881}]^+$ and hexanoic acid, which demonstrated a greater synergy with tunnel 2. The substrate (D-glucose, input) and product (glucose-6-phosphate, output) also showed higher possibilities via tunnel 2. Conversely, the molecule transport via tunnel 2 displayed only a slight inhibition in hexokinase. The experimental observations align closely with the in-silico analysis of the enzymatic tunnels. Specifically, the differential transport preferences of the DES constituents and other ligands through the hexokinase tunnels correlate with their observed inhibitory effects on yeast growth.

Tunnel 1, as depicted in Fig. 4 and S1 (in Supporting Information), is characterized by its shorter length and higher throughput compared to tunnel 2. These features facilitate the more efficient transport of molecules to the YlHxk active site. Consequently, ligands moving through tunnel 1 can access the catalytic site more readily, potentially impeding the substrate's access. This preferential transport of inhibitory ligands via tunnel 1 can explain the observed inhibition of hexokinase. The DES constituents occupying tunnel 1 likely obstruct the active site's access, thereby inhibiting the enzyme's ability to phosphorylate glucose into glucose-6-phosphate.

Understanding how ligands interact with and move through enzyme structures is important for analyzing the pathways these molecules follow during biocatalysis. The transport tunnels within enzymes play a role in facilitating these interactions and ensuring the structural and kinetic stability of the enzyme (Vonásek et al., 2019). Molecular docking tools can be employed to predict how ligands will interact with the enzyme's active site. These tools calculate the binding affinity energy, which helps in identifying potential interaction sites between the ligand and the enzyme's active regions. Docking simulations provide valuable insights into the positions and orientations that ligands are likely to adopt when bound to the enzyme.

3.2.3. *Molecular docking*

Molecular docking was used to understand better the interactions at the molecular level occurring between the HBD/HBA and hexokinase on the *Yarrowia lipolytica* growth, addressing the binding energies, types of interactions, and specific amino acids residues involved (Almeida et al., 2021; Quental et al., 2015), as depicted in Figs. 5 and 6. Generally, the interactions between ligands and amino acids can be hydrogen bonding, and hydrophobic, electrostatic, and van der Waals interactions. The absolute value of affinity (kcal·mol^{-1}) of each ligand to YlHxk, best binding pose and docking affinities, and type of interaction and geometry distance (Å), are reported in Table S4. In contrast, the molecular interaction diagrams are exhibited in Figures S2 to S4 (in Supporting Information).

The affinity energy values obtained from molecular docking provide valuable insights into how ligands interact with enzyme structures. Higher absolute affinity energy values typically indicate stronger interactions between the ligand and the enzyme, which can promote conformational changes within the protein structure and potentially inhibit microbial growth (Barbosa et al., 2019b). It was observed that the docking affinity energies for the HBA-forming cations transported through tunnel 1 in the YlHxk enzyme decreased in the same order as yeast growth inhibition. Specifically, the affinity energy values for these cations were as follows (Table S4): $[N_{8888}]^+$ (-5.3 kcal·mol^{-1}), $[N_{4444}]^+$ (-4.5 kcal·mol^{-1}), and $[Ch]^+$ (-3.5 kcal·mol^{-1}). This trend suggests that cations with higher affinity energies interact more strongly with the enzyme, leading to greater conformational changes that can hinder the enzyme's function, thereby reducing microbial growth. Furthermore, as reported by Ríos (De Los Ríos et al., 2011) and Tsunashima (Tsunashima and Sugiya, 2007), an increase in the cation's alkyl chain length and hydrophobicity generally leads to a reduction in the substrate's accessibility to the enzyme's active site. This is because longer and more hydrophobic alkyl chains create a more substantial barrier, making it difficult for the substrate to reach and interact with the active site of the enzyme.

The hydrophobicity of the HBA-forming cations was evaluated by the logarithm of the octanol-water distribution coefficient, log K_{ow}. In our study, the log K_{ow} values for the cations that were preferentially transported through tunnel 1 in the YlHxk enzyme followed the order: $[N_{8888}]^+$ (9.57) > $[N_{4444}]^+$ (1.71) > $[Ch]^+$ (-5.16). This trend aligns with our experimental data, suggesting that more hydrophobic cations are more effective at blocking access to the YlHxk active site, thereby inhibiting enzyme function and reducing microbial growth. The $[N_{8888}]^+$ cation, with the highest log K_{ow}, exhibited the higher number

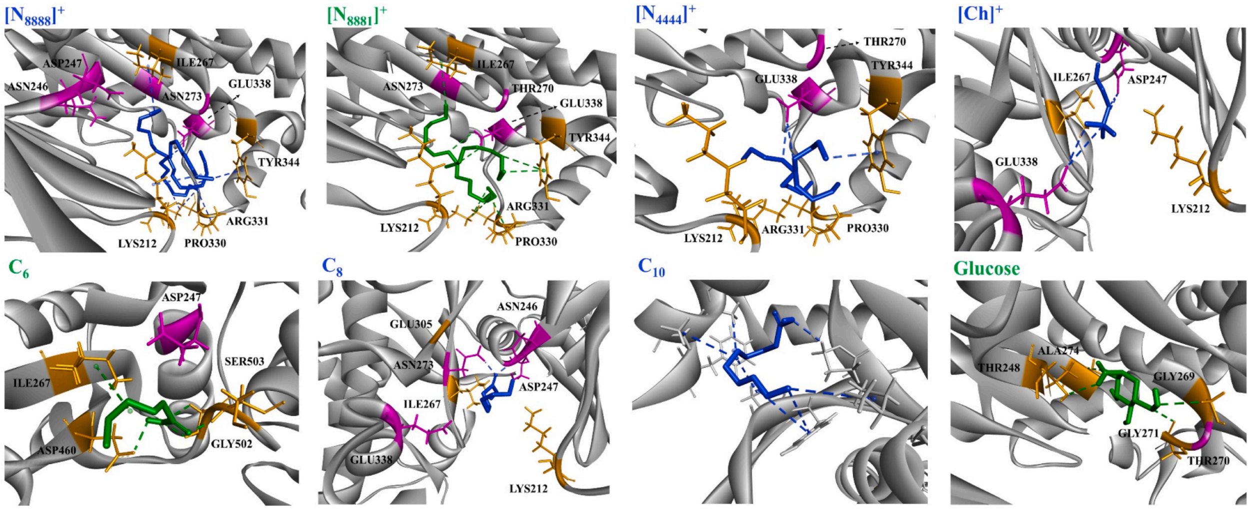

Fig. 5. : Docking pose with the lowest absolute value of affinity (kcal/mol) between HBA-forming cation, HBD, and subtracts/product with the enzyme active site amino acids (pink): ligands transported through tunnel 1 (blue) and tunnel 2 (green).

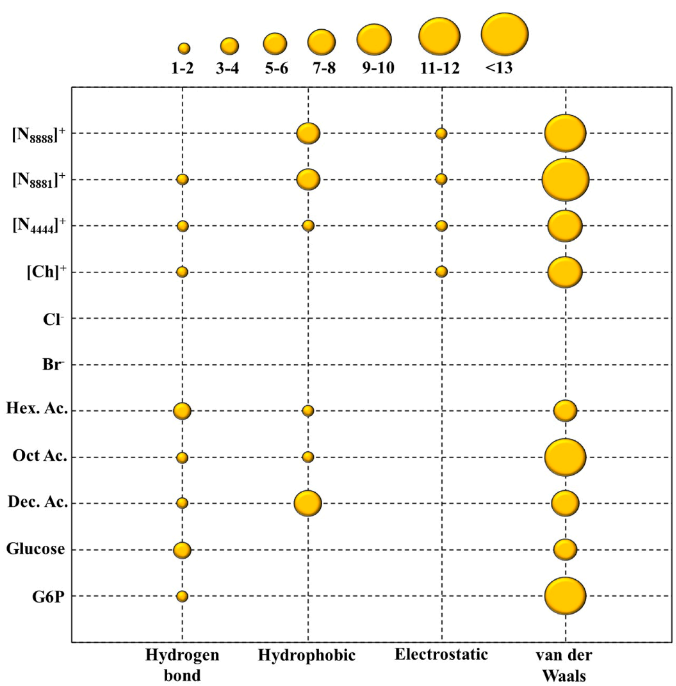

Fig. 6. : Interactions (hydrogen bond, hydrophobic, electrostatic, and van der Waals) between receptor (Hexokinase from *Y. lipolytica*) and ligands (HBA (cations and anions), HBD (hexanoic acid – Hex. Ac.; octanoic acid – Oct. Ac.; decanoic acid – Dec. Ac.), substrate (Glucose), and product (glucose 6-phosphate – G6P) from molecular docking. The usage incidence (amount of interactions) is represented by the size of the circles, which proportionally increases as follows: [1–2] < [3–4] < [5–6] < [7–8] < [9–10] < [11–12] < [<13].

of interactions with the amino acids at the YlHxk active site, namely Glu338 (electrostatic), Asp247 (van der Waals), Asn246 (van der Waals), and Thr270 (van der Waals). For the $[N_{4444}]^+$ cation, interactions were observed with two amino acids related to the enzyme's catalytic site, specifically Glu338 (electrostatic and hydrogen bond) and Thr270 (van der Waals). The $[Ch]^+$ cation, despite its lower hydrophobicity, formed interactions with Glu338 and Asp247, both by electrostatic interactions and hydrogen bonds. Our findings are consistent with the results of Barbosa et al (Barbosa et al., 2019b)., who examined the impact of phosphonium-based ionic liquids on the activity of lipase *from Burkholderia cepacia*. Their study found that cations with higher hydrophobicity and absolute values of affinity energy caused increased inactivation of the enzyme. This suggests a common mechanism where hydrophobic cations with strong interactions at the active site disrupt the enzyme's function, thereby impeding microbial growth.

Regarding the interactions between HBDs and the amino acids located in the active site of YlHxk, interestingly, it was not observed a direct relationship between the chain length of fatty acids and their interactions with the active site amino acids. Specifically, decanoic acid did not interact with the active site, whereas hexanoic acid and octanoic acid demonstrated one and four interactions, respectively. Despite these interaction differences, the yeast growth reduction followed a clear pattern, with the smallest fatty acid, hexanoic acid, leading to the least growth inhibition, followed by octanoic acid, and the longest, decanoic acid, causing the most significant inhibition. This trend aligns with the increasing hydrophobicity and absolute values of affinity energies (in $kcal{\cdot}mol^{-1}$) of the HBDs as the chain length increases, as follows: hexanoic acid (-3.4, $\log K_{ow} = 2.05$) < octanoic acid (-3.8, $\log K_{ow} = 3.03$) < decanoic acid (-4.4, $\log K_{ow} = 4.02$). These properties correlate with the higher inhibition of the YlHxk enzyme and, consequently, lower yeast growth. These findings suggest that the increased hydrophobicity and affinity energy of longer-chain fatty acids contribute to more significant enzyme inhibition.

Further computational analysis revealed that HBA and HBD transported through tunnel 2 exhibited specific binding to the enzyme's active site. Notably, the $[N_{8881}]^+$ cation displayed interactions with three key amino acids: Glu338, Thr270, and Asn273. In contrast, hexanoic acid, along with the glucose and glucose-6-phosphate substrates, only interacted with Asn273 (via van der Waals forces). This distinct binding pattern to Asn273 might explain their lower inhibitory effect on the cell growth. Conversely, ligands using tunnel 1 did not show any affinity for Asn273, which could suggest different inhibitory mechanisms or less direct inhibition of the enzyme's active site. These results corroborate with previous molecular docking studies, such as those by Toledo et al (Toledo et al., 2019)., where the effectiveness of DES on laccase activation was linked to specific amino acid interactions. Similarly, the interactions between DES components and amino acids within tunnel 1 could lead to conformational changes in the enzyme structure, potentially mitigating competitive inhibition by altering the enzyme's form or accessibility to the substrate.

The interactions between the chloride (Cl^-) and bromide (Br^-) anions and the YlHxk enzyme were also evaluated, focusing on their potential allosteric effects. As presented in Table S4, the affinity energies between YlHxk and the Cl^- and Br^- anions were relatively low, −1.2 and −1.1 kcal·mol^{-1}, respectively. These values suggest weaker interactions compared to the cations studied. Additionally, the log K_{ow} values were 0.54 for Cl^- and 0.63 for Br^-. These anions exhibit a trend where increasing hydrophobicity is associated with higher enzyme inhibition, aligning with the previously observed effects of other hydrophobic ions. Cl^- and Br^- anions possess high charge densities and were found to be located significantly further from the YlHxk active site compared to the cations and fatty acids. This spatial separation implies a more favorable environment for allosteric inhibition rather than direct competitive inhibition at the active site. The Cl^- and Br^- anions were located near allosteric site 1 (Figure S5 in support information), which was identified as having the highest probability of being the principal allosteric site of the hexokinase enzyme. Supporting this hypothesis, Zhao et al (Zhao, 2016). highlighted that these anions, categorized as chaotropic, can disrupt and inactivate various enzymes through mechanisms that often involve destabilization of protein structure and function. Our findings are consistent with this view, underscoring the inhibitory potential of these anions on YlHxk.

4. Conclusion

DES offer a promising avenue for enhancing the efficiency and sustainability of biocatalytic processes. The results obtained reveal that the presence of DES in the culture medium generally inhibited *Y. lipolytica* growth. However, an exception was noted with the DES composed of $[N_{8881}]$Cl and hexanoic acid, which showed growth values comparable to the control. To understand these inhibitory effects at a molecular level, we employed computational tools to analyze the interactions between DES components and the enzyme hexokinase (YlHxk) from *Y. lipolytica*. Structural analysis of YlHxk identified four favorable tunnels that facilitate ligand transport from the enzyme surface to the active site. Tunnel 1 was the most favorable pathway for transporting several HBA cations ($[N_{8888}]^{+}$, $[N_{4444}]^{+}$, and $[Ch]^{+}$) and the HBDs (octanoic and decanoic acids). Ligands using Tunnel 1 were associated with the lowest yeast growth values, suggesting potential for competitive inhibition at the enzyme's active site. Ligands transported by tunnel 2, such as $[N_{8881}]^{+}$ and hexanoic acid, did not significantly inhibit growth, along with glucose and glucose 6-phosphate. The longer length of Tunnel 2 likely reduces competition between ligands and substrates, facilitating efficient transport without significant inhibition. Molecular docking analyses provided further insights into the interactions between DES components and YlHxk. Ligands utilizing Tunnel 2 were the only ones forming van der Waals interactions with the ASN273 amino acid in the YlHxk active site. This unique interaction pattern may contribute to their lower inhibitory effects, aligning with the observed growth data.

The combined experimental and computational approach offered a comprehensive understanding of how DES components influence Y. lipolytica growth and YlHxk enzyme activity. The identification of specific transport pathways and interactions within the enzyme highlights the complex dynamics between DES and biological systems. This knowledge enhances the potential for designing DES that optimize biocatalytic processes, leading to more efficient and sustainable biotechnological applications.

CRediT authorship contribution statement

Bernardo Dias Ribeiro: Writing – review & editing, Visualization, Validation, Data curation. **Filipe Smith Buarque:** Writing – original draft, Visualization, Methodology, Investigation, Formal analysis, Conceptualization. **Maria Alice Z. Coelho:** Supervision, Project administration, Funding acquisition. **Mara G. Freire:** Writing – review & editing, Validation, Supervision. **Matheus M. Pereira:** Writing – review & editing, Supervision, Conceptualization.

Declaration of Competing Interest

The authors declare that they have no known competing financial interests or personal relationships that could have appeared to influence the work reported in this paper.

Acknowledgements

This work was financed by national funds through the National Council for Scientific and Technological Development (CNPq); Coordination of Improvement of Higher-Level Personnel (CAPES); and Foundation for Research Support and Technological Innovation of the State of Rio de Janeiro (FAPERJ). This work was developed within the scope of the project CICECO-Aveiro Institute of Materials, UIDB/50011/2020 (DOI 10.54499/UIDB/50011/2020), UIDP/50011/2020 (DOI 10.54499/UIDP/50011/2020) & LA/P/0006/2020 (DOI 10.54499/LA/P/0006/2020), financed by national funds through the FCT/MCTES (PIDDAC). Matheus M. Pereira acknowledges the financial support of FCT, Portugal, within the projects DOI:10.54499/UIDB/00102/2020 (Base funding) and DOI: 10.54499/UIDP/00102/2020 (Programmatic funding). F.S. Buarque acknowledges the grant from FAPERJ: E-26/204.344/2021.

Appendix A. Supporting information

Supplementary data associated with this article can be found in the online version at doi:10.1016/j.jbiotec.2024.11.016.

Data availability

Data will be made available on request.

References

Almeida, L.C., Barbosa, M.S., de Jesus, F.A., Santos, R.M., Fricks, A.T., Freitas, L.S., Pereira, M.M., Lima, Á.S., Soares, C.M.F., 2021. Enzymatic transesterification of coconut oil by using immobilized lipase on biochar: An experimental and molecular docking study. Biotechnol. Appl. Biochem 68, 801–808. https://doi.org/10.1002/bab.1992.

Azevedo, T.S.M., Silva, L.K.B., Lima, Á.S., Pereira, M.M., Franceschi, E., Faria Soares, C. M., 2022. In silico evaluation of enzymatic tunnels in the biotransformation of α-tocopherol esters. Front Bioeng. Biotechnol. 9. https://doi.org/10.3389/fbioe.2021.805059.

Barbosa, M.S., Freire, C.C.C., Almeida, L.C., Freitas, L.S., Souza, R.L., Pereira, E.B., Mendes, A.A., Pereira, M.M., Lima, Á.S., Soares, C.M.F., 2019a. Optimization of the enzymatic hydrolysis of Moringa oleifera Lam oil using molecular docking analysis for fatty acid specificity. Biotechnol. Appl. Biochem 66, 823–832. https://doi.org/10.1002/bab.1793.

Barbosa, M.S., Freire, C.C.C., Souza, R.L., Cabrera-Padilla, R.Y., Pereira, M.M., Freire, M. G., Lima, Á.S., Soares, C.M.F., 2019b. Effects of phosphonium-based ionic liquids on the lipase activity evaluated by experimental results and molecular docking. Biotechnol. Prog. 35. https://doi.org/10.1002/btpr.2816.

Barth, G., Gaillardin, C., 1997. Physiology and genetics of the dimorphic fungus Yarrowia lipolytica. FEMS Microbiol Rev. 19, 219–237. https://doi.org/10.1111/j.1574-6976.1997.tb00299.x.

Bisht, M., Mondal, D., Pereira, M.M., Freire, M.G., Venkatesu, P., Coutinho, J.A.P., 2017. Long-term protein packaging in cholinium-based ionic liquids: Improved catalytic activity and enhanced stability of cytochrome c against multiple stresses. Green. Chem. 19, 4900–4911. https://doi.org/10.1039/c7gc02011b.

Buarque, F.S., Carniel, A., Ribeiro, B.D., Coelho, M.A.Z., 2023a. Selective enzymes separation from the fermentation broth of Yarrowia lipolytica using aqueous two-phase system based on quaternary ammonium compounds. Sep Purif. Technol. 324, 124539. https://doi.org/10.1016/j.seppur.2023.124539.

Buarque, F.S., Farias, M.A., Sales, J.C.S., Carniel, A., Ribeiro, B.D., de, V.R., Lopes, O., Castro, A.M., Coelho, M.A.Z., 2023c. Valorization of macauba (Acromia aculeata) for integrated production of lipase by yarrowia lipolytica and biodiesel esters. Fermentation 9, 992–1002. https://doi.org/10.3390/fermentation9120992.

Buarque, F.S., Monteiro e Silva, S.A., Ribeiro, B.D., 2023b. Choline chloride-based deep eutectic solvent as an inhibitor of metalloproteases (collagenase and elastase) in cosmetic formulation. 3 Biotech 13, 219–232. https://doi.org/10.1007/s13205-023-03602-2.

Chaudhary, K.K., Mishra, N., 2016. A review on molecular docking: novel tool for drug discovery, a review on molecular docking: novel tool for drug discovery. JSM Chem. 4, 1029.

Chlipała, P., Janeczko, T., Mazur, M., 2024. Bioreduction of 4′-hydroxychalcone in deep eutectic solvents: optimization and efficacy with various yeast strains. Int J. Mol. Sci. 25, 7152–7169. https://doi.org/10.3390/ijms25137152.

Chong, W., Qi, Y., Ji, L., Zhang, Z., Lu, Z., Nian, B., Hu, Y., 2023. Computer-aided tunnel engineering: a promising strategy for improving lipase applications in esterification reactions. ACS Catal. 67–83. https://doi.org/10.1021/acscatal.3c04491.

Chovancova, E., Pavelka, A., Benes, P., Strnad, O., Brezovsky, J., Kozlikova, B., Gora, A., Sustr, V., Klvana, M., Medek, P., Biedermannova, L., Sochor, J., Damborsky, J., 2012. CAVER 3.0: a tool for the analysis of transport pathways in dynamic protein structures. PLoS Comput. Biol. 8, 1002708. https://doi.org/10.1371/journal.pcbi.1002708.

Ferreira, L.G., Dos Santos, R.N., Oliva, G., Andricopulo, A.D., 2015. Molecular docking and structure-based drug design strategies. Molecules 20, 13384–13421. https://doi.org/10.3390/molecules200713384.

Filipovic, J., Vavra, O., Plhak, J., Bednar, D., Marques, S.M., Brezovsky, J., Matyska, L., Damborsk, J., 2020. CaverDock: a novel method for the fast analysis of ligand transport. IEEE/ACM Trans. Comput. Biol. Bioinf. 17, 1625–1638. https://doi.org/10.1109/TCBB.2019.2907492.

Gao, W.W., Zhang, F.X., Zhang, G.X., Zhou, C.H., 2015. Key factors affecting the activity and stability of enzymes in ionic liquids and novel applications in biocatalysis. Biochem Eng. J. 99, 67–84. https://doi.org/10.1016/j.bej.2015.03.005.

A.N. Hagler, L.C. Mendonqa-Hagler, Yeasts from Marine and Estuarine Waters with Different Levels of Pollution in the State of Rio de Janeiro, Brazil, 1981. ⟨https://journals.asm.org/journal/aem⟩.

Hapeta, P., Szczepańska, P., Neuvéglise, C., Lazar, Z., 2021a. A 37-amino acid loop in the Yarrowia lipolytica hexokinase impacts its activity and affinity and modulates gene expression. Sci. Rep. 11, 6411–6425. https://doi.org/10.1038/s41598-021-85837-8.

Hapeta, P., Szczepańska, P., Witkowski, T., Nicaud, J.M., Crutz-Le Coq, A.M., Lazar, Z., 2021b. The role of hexokinase and hexose transporters in preferential use of glucose over fructose and downstream metabolic pathways in the yeast Yarrowia lipolytica. Int J. Mol. Sci. 22, 9282–9302. https://doi.org/10.3390/ijms22179282.

Huang, Z., Zhu, L., Cao, Y., Wu, G., Liu, X., Chen, Y., Wang, Q., Shi, T., Zhao, Y., Wang, Y., Li, W., Li, Y., Chen, H., ZhangChen, G., Zhang, J., 2011. ASD: a comprehensive database of allosteric proteins and modulators. Nucleic Acids Res 39, 663–669. https://doi.org/10.1093/nar/gkq1022.

Kaushik, S., Marques, S.M., Khirsariya, P., Paruch, K., Libichova, L., Brezovsky, J., Prokop, Z., Chaloupkova, R., Damborsky, J., 2018. Impact of the access tunnel engineering on catalysis is strictly ligand-specific. FEBS J. 285, 1456–1476. https://doi.org/10.1111/febs.14418.

Kim, S.M., Kang, S.H., Jeon, B.W., Kim, Y.H., 2024. Tunnel engineering of gas-converting enzymes for inhibitor retardation and substrate acceleration. Bioresour. Technol. 394, 130248. https://doi.org/10.1016/j.biortech.2023.130248.

Kuser, P.R., Krauchenco, S., Antunes, O.A.C., Polikarpov, I., 2000. The high resolution crystal structure of yeast hexokinase PII with the correct primary sequence provides new insights into its mechanism of action. J. Biol. Chem. 275, 20814–20821. https://doi.org/10.1074/jbc.M910412199.

Van Lam Van, T., Heindl, M.R., Schlutt, C., Böttcher-Friebertshäuser, E., Bartenschlager, R., Klebe, G., Brandstetter, H., Dahms, S.O., Steinmetzer, T., 2021. The basicity makes the difference: improved canavanine-derived inhibitors of the proprotein convertase furin. ACS Med Chem. Lett. 12, 426–432. https://doi.org/10.1021/acsmedchemlett.0c00651.

Li, Y., Sen, D., 1998. The modus operandi of a DNA enzyme: enhancement of substrate basicity. Cell Chem. Biol. 5, 1–12. ⟨http://biomednet.com/elecref/1074552100500001⟩.

De Los Ríos, A.P., Hernández Fernández, F.J., Gómez, D., Rubio, M., Víllora, G., 2011. Biocatalytic transesterification of sunflower and waste cooking oils in ionic liquid media. Process Biochem. 46, 1475–1480. https://doi.org/10.1016/j.procbio.2011.03.021.

Lu, Z., Li, X., Zhang, R., Yi, L., Ma, Y., Zhang, G., 2019b. Tunnel engineering to accelerate product release for better biomass-degrading abilities in lignocellulolytic enzymes. Biotechnol. Biofuels 12, 275–292. https://doi.org/10.1186/s13068-019-1616-3.

Lu, S., Shen, Q., Zhang, J., 2019a. Allosteric methods and their applications: facilitating the discovery of allosteric drugs and the investigation of allosteric mechanisms. Acc. Chem. Res 492–500. https://doi.org/10.1021/acs.accounts.8b00570.

Marques, S.M., Daniel, L., Buryska, T., Prokop, Z., Brezovsky, J., Damborsky, J., 2017. Enzyme tunnels and gates as relevant targets in drug design. Med Res Rev. 37, 1095–1139. https://doi.org/10.1002/med.21430.

Matoba, Y., Oda, K., Muraki, Y., Masuda, T., 2021. The basicity of an active-site water molecule discriminates between tyrosinase and catechol oxidase activity. Int J. Biol. Macromol. 183, 1861–1870. https://doi.org/10.1016/j.ijbiomac.2021.05.206.

Maugeri, Z., Domínguez De María, P., 2014. Whole-cell biocatalysis in deep-eutectic-solvents/aqueous mixtures. ChemCatChem 6, 1535–1537. https://doi.org/10.1002/cctc.201400077.

Mohedano, M.T., Konzock, O., Chen, Y., 2022. Strategies to increase tolerance and robustness of industrial microorganisms. Synth. Syst. Biotechnol. 7, 533–540. https://doi.org/10.1016/j.synbio.2021.12.009.

Morris, G.M., Ruth, H., Lindstrom, W., Sanner, M.F., Belew, R.K., Goodsell, D.S., Olson, A.J., 2009. Software news and updates AutoDock4 and AutoDockTools4: automated docking with selective receptor flexibility. J. Comput. Chem. 30, 2785–2791. https://doi.org/10.1002/jcc.21256.

Nicaud, J.M., 2012. Yarrowia lipolytica. Yeast 29, 409–418. https://doi.org/10.1002/yea.2921.

Panić, M., Cvjetko Bubalo, M., Radojčić Redovniković, I., 2021. Designing a biocatalytic process involving deep eutectic solvents. J. Chem. Technol. Biotechnol. 96, 14–30. https://doi.org/10.1002/jctb.6545.

Pätzold, M., Siebenhaller, S., Kara, S., Liese, A., Syldatk, C., Holtmann, D., 2019. Deep eutectic solvents as efficient solvents in biocatalysis. Trends Biotechnol. 37, 943–959. https://doi.org/10.1016/j.tibtech.2019.03.007.

Pernak, J., Sobaszkiewicz, K., Mirska, I., 2003. Anti-microbial activities of ionic liquids. Green. Chem. 5, 52–56. https://doi.org/10.1039/b207543c.

Pinto, G.P., Vavra, O., Marques, S.M., Filipovic, J., Bednar, D., Damborsky, J., 2021. Screening of world approved drugs against highly dynamical spike glycoprotein of SARS-CoV-2 using CaverDock and machine learning. Comput. Struct. Biotechnol. J. 19, 3187–3197. https://doi.org/10.1016/j.csbj.2021.05.043.

Planas-Iglesias, J., Marques, S.M., Pinto, G.P., Musil, M., Stourac, J., Damborsky, J., Bednar, D., 2021. Computational design of enzymes for biotechnological applications. Biotechnol. Adv. 47, 107696. https://doi.org/10.1016/j.biotechadv.2021.107696.

Pravda, L., Berka, K., Svobodová Vařeková, R., Sehnal, D., Banáš, P., Laskowski, R.A., Koča, J., Otyepka, M., 2014. Anatomy of enzyme channels. BMC Bioinforma. 15, 379–395. https://doi.org/10.1186/s12859-014-0379-x.

Prokop, Z., Gora, A., Brezovsky, J., Chaloupkova, R., 2012. Engineering of protein tunnels: Keyhole-lock-key model for catalysis by the enzymes with active sites. Protein Eng. Handb. 3, 421–464.

Qian, F., Liu, H.Y., Yu, S.R., Zhang, Y., Wang, P., 2023. New strategy for effective biosynthesis of chiral aryl alcohols: co-cultivation microbe with natural deep-eutectic solvent. ACS Sustain Chem. Eng. 11, 4441–4449. https://doi.org/10.1021/acssuschemeng.2c07430.

Quental, M.V., Passos, H., Kurnia, K.A., Coutinho, J.A.P., Freire, M.G., 2015. Aqueous biphasic systems composed of ionic liquids and acetate-based salts: phase diagrams, densities, and viscosities. J. Chem. Eng. Data 60, 1674–1682. https://doi.org/10.1021/je501044u.

Rodrigues, C. de A., Barbosa, M.S., dos Santos, J.C.B., Lisboa, M.C., Souza, R.L., Pereira, M.M., Lima, Á.S., Soares, C.M.F., 2021. Computational and experimental analysis on the preferential selectivity of lipases for triglycerides in Licuri oil. Bioprocess Biosyst. Eng. 44, 2141–2151. https://doi.org/10.1007/s00449-021-02590-y.

Rodrigues, C.A., Santos, J.C.B., Barbosa, M.S., Lisboa, M.C., Souza, R.L., Mendes, A.A., Pereira, M.M., Lima, A.S., Soares, C.M.F., 2024. Extending the computational and experimental analysis of lipase active site selectivity. Bioproces Biosyst. Eng. 47, 313–323.

Santos, A.G., Buarque, F.S., Ribeiro, B.D., Coelho, M.A.Z., 2022. Extractive fermentation for the production and partitioning of lipase and citric acid by Yarrowia lipolytica. Process Biochem. 122, 374–385. https://doi.org/10.1016/j.procbio.2022.09.011.

Santos, A.G., Ribeiro, B.D., Alviano, D.S., Coelho, M.A.Z., 2014. Toxicity of ionic liquids toward microorganisms interesting to the food industry. RSC Adv. 4, 37157–37163. https://doi.org/10.1039/c4ra05295a.

Shishov, A., Dubrovsky, I., Kirichenko, S., Bulatov, A., 2022. Behavior of quaternary ammonium salts and terpenoids-based deep eutectic solvents in aqueous phase. J. Mol. Liq. 347, 117987. https://doi.org/10.1016/j.molliq.2021.117987.

Singh, N., Chaput, L., Villoutreix, B.O., 2021. Virtual screening web servers: Designing chemical probes and drug candidates in the cyberspace. Brief. Bioinf. 22, 1790–1818. https://doi.org/10.1093/bib/bbaa034.

Stourac, J., Vavra, O., Kokkonen, P., Filipovic, J., Pinto, G., Brezovsky, J., Damborsky, J., Bednar, D., 2019. Caver Web 1.0: Identification of tunnels and channels in proteins and analysis of ligand transport. Nucleic Acids Res 47, W414–W422. https://doi.org/10.1093/nar/gkz378.

Tian, H., Xiao, S., Jiang, X., Tao, P., 2023. PASSer: Fast and accurate prediction of protein allosteric sites. Nucleic Acids Res 51, 427–431. https://doi.org/10.1093/nar/gkad303.

Toledo, M.L., Pereira, M.M., Freire, M.G., Silva, J.P.A., Coutinho, J.A.P., Tavares, A.P.M., 2019. Laccase activation in deep eutectic solvents. ACS Sustain Chem. Eng. 7, 11806–11814. https://doi.org/10.1021/acssuschemeng.9b02179.

Trott, O., Olson, A.J., 2010. AutoDock Vina: Improving the speed and accuracy of docking with a new scoring function, efficient optimization, and multithreading. J. Comput. Chem. 31, 455–461. https://doi.org/10.1002/jcc.21334.

Tsunashima, K., Sugiya, M., 2007. Physical and electrochemical properties of low-viscosity phosphonium ionic liquids as potential electrolytes. Electrochem Commun. 9, 2353–2358. https://doi.org/10.1016/j.elecom.2007.07.003.

Vavra, O., Filipovic, J., Plhak, J., Bednar, D., Marques, S.M., Brezovsky, J., Stourac, J., Matyska, L., Damborsky, J., 2019. CaverDock: a molecular docking-based tool to analyse ligand transport through protein tunnels and channels. Bioinformatics 35, 4986–4993. https://doi.org/10.1093/bioinformatics/btz386.

Vonásek, V., Jurčík, A., Furmanová, K., Kozlíková, B., 2019. Sampling-based motion planning for tracking evolution of dynamic tunnels in molecular dynamics simulations. J. Intell. Robot. Syst.: Theory Appl. 93, 763–785. https://doi.org/10.1007/s10846-018-0877-6.

Xiao, S., Alshahrani, M., Gupta, G., Tao, P., Verkhivker, G., 2023. Markov state models and perturbation-based approaches reveal distinct dynamic signatures and hidden allosteric pockets in the emerging SARS-Cov-2 spike omicron variant complexes with the host receptor: the interplay of dynamics and convergent evolution modulates allostery and functional mechanisms. J. Chem. Inf. Model 63, 5272–5296. https://doi.org/10.1021/acs.jcim.3c00778.

Xiao, S., Tian, H., Tao, P., 2022. PASSer2.0: accurate prediction of protein allosteric sites through automated machine learning. Front Mol. Biosci. 9. https://doi.org/10.3389/fmolb.2022.879251.

Yang, T.X., Zhao, L.Q., Wang, J., Song, G.L., Liu, H.M., Cheng, H., Yang, Z., 2017. Improving whole-cell biocatalysis by addition of deep eutectic solvents and natural

deep eutectic solvents. ACS Sustain Chem. Eng. 5, 5713–5722. https://doi.org/10.1021/acssuschemeng.7b00285.
Zeng, C., Fromm, H.J., 1995. Active site residues of human brain hexokinase as studied by site-specific mutagenesis. J. Biol. Chem. 270, 10509–10513. https://doi.org/10.1074/jbc.270.18.10509.
Zhao, H., 2016. Protein stabilization and enzyme activation in ionic liquids: specific ion effects. J. Chem. Technol. Biotechnol. 91, 25–50. https://doi.org/10.1002/jctb.4837.